A New Flux Splitting Scheme

MENG-SING LIOU AND CHRISTOPHER J. STEFFEN, JR.

Internal Fluid Mechanics Division, NASA Lewis Research Center, Cleveland, Ohio 44135

A new flux splitting scheme is proposed. The scheme is remarkably simple and yet its accuracy rivals, and in some cases surpasses, that of Roe's solver in the Euler and Navier–Stokes solutions carried out in this study. The scheme is robust and converges as fast as the Roe splitting. We propose an appropriately defined cell-face advection Mach number using values from the two straddling cells via associated characteristic speeds. This interface Mach number is then used to determine the upwind extrapolation for the convective quantities. Accordingly, the name of the scheme is coined as the advection upstream splitting method (AUSM). We also introduce a new pressure splitting which is shown to behave successfully, yielding much smoother results than other existing pressure splittings. Of particular interest is the supersonic blunt body problem in which the Roe scheme gives anomalous solutions. The AUSM produces correct solutions without difficulty for a wide range of flow conditions as well as grids. © 1993 Academic Press, Inc.

1. INTRODUCTION

Maximizing both accuracy and efficiency has been the primary goal for designing an algorithm in numerical analysis. This is especially important for solution of complex 3D problems described by the Navier–Stokes equations which may include equations for a turbulence model and/or chemical species. Recently upwind schemes have become well received for the sound theoretical basis of characteristic theory for hyperbolic systems and thus for their capability of capturing discontinuities. Furthermore, many advanced shock capturing techniques such as TVD are based on upwind schemes.

Several prominent flux splitting schemes have been compared in the literature. Liou and Van Leer [1] tested three techniques, namely the Steger–Warming (SWS), Van Leer (VLS) and Roe splittings (RS), for a variety of problems regarding their accuracy and efficiency. Osher's splitting (OS) has recently been compared with Van Leer's by Koren [2] and extended to both equilibrium and non-equilibrium chemistry by Suresh and Liou [3, 4]. Flux-vector splitting (FVS) such as VLS and SWS has proved to be a simple and useful technique for arriving at upwind differencing and is preeminently suited for use in implicit schemes. Unfor-

tunately, the simplicity of these two splittings comes at a price of reduced accuracy due to numerical diffusion. Flux-difference splitting (FDS) such as RS and OS, however, has shown to be very accurate and particularly well suited for explicit upwind formulations. Nevertheless, the increased accuracy is accompanied with an increased operation count and complexity in arriving at the complete linearization of flux formulas for the implicit schemes. Hence, the simplicity of FVS is still motivating researchers to investigate new ways of splitting and combinations of FVS and FDS that do away with the problem of numerical diffusion with only a small (if any) increase in complexity.

In SWS, glitches exist at a point where eigenvalues change sign, such as a sonic or a shock point. Although fixes have been proposed, it is generally agreed that the other three splittings are preferred within the framework of upwind discretization. As pointed out by Van Leer himself [5], the Van Leer splitting fails to recognize the contact discontinuity, leading to excessive numerical diffusion. As a result, significant error appears in the viscous region which cannot be simply cured by reducing grid size and/or using higher order differencing. This fact had largely gone unnoticed until 1987 when Van Leer again brought this deficiency to the attention of researchers [6]. Subsequently, several efforts have been attempted to improve the original Van Leer scheme, in particular by Hänel and Schwane *et al.* [7, 8]. Van Leer, recently based upon [8], has made a drastic improvement [9], in which the temperature distribution of a hypersonic conic flow is predicted as accurately as using Roe's splitting. However, a pressure glitch is accompanied with this new scheme. Another approach was suggested by Liou and Steffen [11] and Coirier and Van Leer [18] to include higher order polynomial expansions in the split fluxes in order to yield vanishing value at $M = 0$. However, this is found to be less stable or oscillatory.

Hence, the current research is motivated by the desire to combine the efficiency of FVS and the accuracy of FDS. In this paper, we will present a new flux splitting scheme (details given in the next section) that is remarkably simple

and accurate, yielding vanishing numerical diffusivity at the stagnation. In a variety of Euler and Navier–Stokes calculations performed, the accuracy of the present scheme is shown to be rivaling that of Roe's splitting. Also, the scheme has no matrix operation, is much simpler to construct, and thus is more efficient. Unlike Roe's splitting, the scheme does not involve differentiation of fluxes—Jacobian matrix; hence it is not subject to the difficulty arising from the differentiation. Specifically, the pressure derivatives with respect to density and internal energy do not explicitly appear in the flux formulas. This feature is especially desirable for the gas with a general equation of state since numerical approximation of a steep variation of thermodynamic states often causes difficulties. The scheme is a mixture, but it has the advantages of both flux-vector and flux-difference splittings.

2. ANALYSIS

Motivation

It would seem helpful at the outset to give reasons for the effort of researching a new flux function, while one may argue that current methods are quite satisfactory for predicting many complex flows. Unfortunately, some recent discoveries also indicate deficiencies of these methods in the calculation of some simple flows. One example is the supersonic viscous flow over a cone, wherein a very thin viscous layer is attached to the cone surface and a shock wave stands away from the wall; for details see Section 4, Case 1. This is an ideal problem for testing the capability of capturing a shock discontinuity together with a sharp-gradient boundary layer. Thus, an algorithm must be designed to minimize the numerical smearing at the locations where an eigenvalue changes sign (at the shock) or approaches zero (in the boundary layer). For example, Van Leer's splitting [5] can represent a shock profile well, while it greatly diffuses the boundary layer. Figure 1 shows that the split flux deviates the most from the true flux at $M = 0$, thereby creating enormous diffusion. As a result of this nonvanishing flux at $M = 0$, the boundary layer is significantly broadened, yielding incorrect pressure and temperature distributions, as seen in Figs. 2a and b. Several fixes for the Van Leer splitting have been proposed to resolve this issue of nonvanishing mass diffusion. Two types, in particular, have proved the most successful to data:

1. High order polynomial expansions (HOPE) of the flux vector given by the authors [11], and a slight variation by Coirier and Van Leer [18], and

2. Hybrid FVS technique first proposed by Hänel *et al.* [7, 8] and later extended by Van Leer [9].

The former, while capable of generating a vanishing mass diffusion and producing excellent results for the conical 1D model problem, yields nonphysical oscillatory solutions in
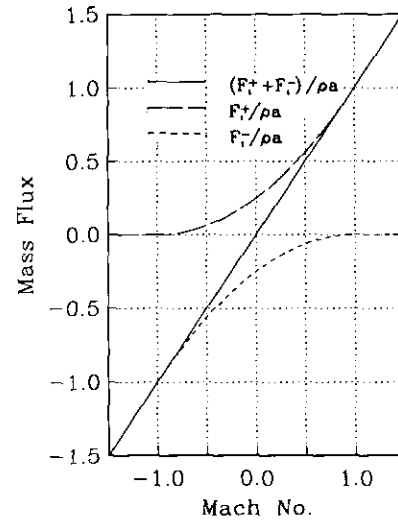

FIG. 1. Mass flux splitting of the Van Leer scheme.

2D problems. This is primarily due to the improper sign of the eigenvalues of the flux Jacobian in a small region in $-1 \leqslant M \leqslant 1$. The latter, while predicting correct boundary-layer thickness and wall temperature (see Fig. 3b), yields glitchs in the pressure near the edge of the boundary layer, see Fig. 3a. Furthermore, an incorrect sign of the normal velocity component near the wall will be seen later in Fig. 5. Clearly both improvements are still unacceptable.

The Roe splitting has been commonly accepted as one of the most accurate techniques available today. However, the setup cost of this method requires $O(n^2)$ operations per grid point in each iteration, where n is the number of equations. Thus a heavy price is paid for the accuracy obtained. Several attempts have been made to reduce the computational cost by replacing the Roe matrix. Roe [19] proposed using the scalar amplitude–square weighted wave speed of Harten and Lax. Unfortunately, the scheme suffers from a stability problem in which the L_∞ norm of the residual can be driven down only an order of magnitude on this test problem. One scheme essentially equal to the RS in accuracy is the Osher scheme. The major computation cost in this scheme lies in the determination of the intermediate states connecting the two states of the neighboring grid points. Again, $O(n^2)$ operations are required.

Based on the conclusions drawn from many past researches, one wonders whether it is possible to arrive at an upwind scheme with the following properties: (1) accurate; (2) simple, requiring only $O(n)$ operations; and (3) stable, for a wide range of problems. It is this question that motivates the research reported in the present paper.

A New Upwind Scheme—AUSM

We turn now to the detailed derivation of the method. To exemplify the concept, let us consider the two-dimensional system of Euler equations for perfect gas,
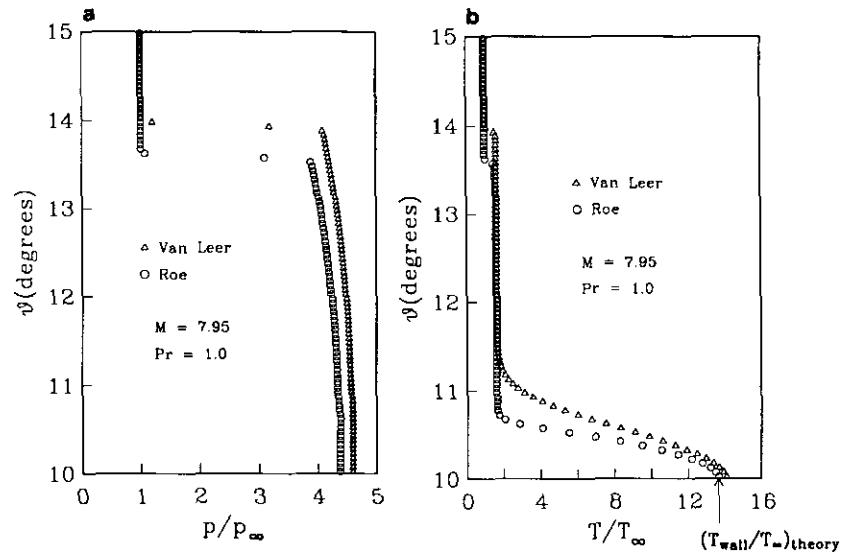
FIG. 2. Hypersonic conical flow, first-order accurate results: (a) pressure profile and (b) temperature profile, using the Van Leer and Roe splittings. Note the diffused boundary layer of the Van Leer solution and its effect on shock location.
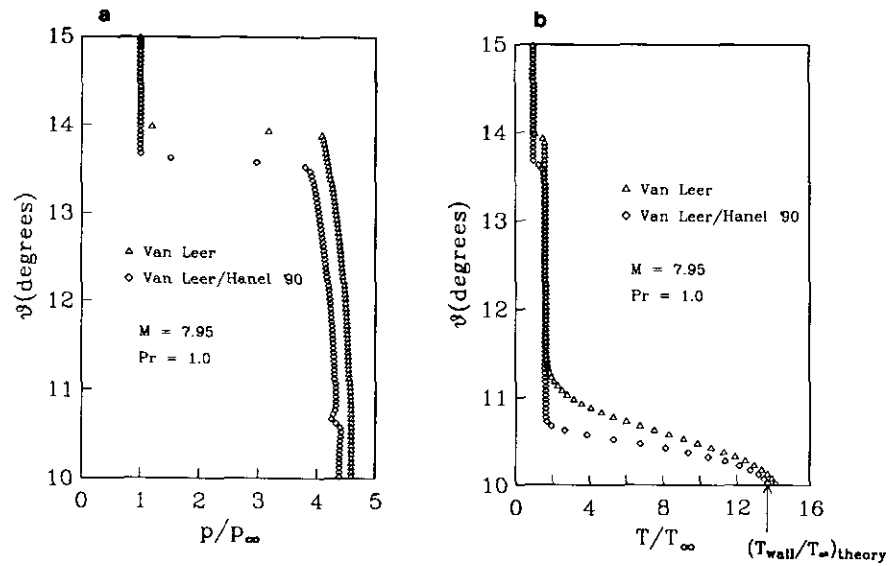

FIG. 3. Hypersonic conical flow, first order accurate results: (a) pressure profile and (b) temperature profile, using the Van Leer and the modified (Hänel/Van Leer) splittings.

$$\frac{\partial \mathbf{U}}{\partial t} + \frac{\partial \mathbf{F}}{\partial x} + \frac{\partial \mathbf{G}}{\partial y} = 0 \qquad (1)$$

where $\mathbf{U}^T = (\rho,\ \rho u,\ \rho v,\ \rho E)$, the inviscid fluxes $\mathbf{F}^T = (\rho u,\ \rho u^2 + p,\ \rho uv,\ \rho uH)$, $\mathbf{G}^T = (\rho u,\ \rho vu,\ \rho v^2 + p,\ \rho vH)$, and the specific total energy $E = e + 1/2(u^2 + v^2) = H - p/\rho$.

The first step is to recognize that the inviscid flux vector F consists of two physically distinct parts, namely *convective* and *pressure* terms:

$$\mathbf{F} = \begin{pmatrix} \rho \\ \rho u \\ \rho v \\ \rho H \end{pmatrix} u + \begin{pmatrix} 0 \\ p \\ 0 \\ 0 \end{pmatrix} = \mathbf{F}^{(c)} + \begin{pmatrix} 0 \\ p \\ 0 \\ 0 \end{pmatrix}. \qquad (2)$$

The convective terms can now be considered as passive scalar quantities convected by a *suitably* defined velocity u at the cell interface. On the other hand, the pressure flux terms are governed by the acoustic wave speeds. Thus we propose to discretize the two components separately. At an interface $L < \frac{1}{2} < R$, the convective terms can be effectively written as

$$\mathbf{F}^{(c)}_{1/2} = u_{1/2} \begin{pmatrix} \rho \\ \rho u \\ v \\ \rho H \end{pmatrix}_{L/R} = M_{1/2} \begin{pmatrix} \rho a \\ \rho a u \\ \rho a v \\ \rho a H \end{pmatrix}_{L/R}, \qquad (3)$$

where

$$(\bullet)_{L/R} = \begin{cases} (\bullet)_L, & \text{if } M_{1/2} \geqslant 0, \\ (\bullet)_R, & \text{otherwise.} \end{cases} \qquad (4)$$

Note that this development opens up a whole new family of schemes based upon the formulation chosen for the advective velocity $M_{1/2}$. One successful choice is to represent this velocity as a combination of the wave speeds $(M \pm 1)$ traveling towards the interface $(\frac{1}{2})$ from the adjacent L and R cells. This is formally written, by combining the contributions from both the "left" and "right" states, as

$$M_{1/2} = M_L^+ + M_R^-. \qquad (5)$$

Various ways of defining the split Mach numbers $M^{\pm}$ exist. In this paper we choose to use the Van Leer splitting [5].

$$M^{\pm} = \begin{cases} \pm \frac{1}{4}(M \pm 1)^2, & \text{if } |M| \leqslant 1; \\ \frac{1}{2}(M \pm |M|), & \text{otherwise.} \end{cases} \qquad (6)$$

We turn now to the pressure term by writing

$$p_{1/2} = p_L^+ + p_R^-. \qquad (7)$$

Again the pressure splitting is weighted using the polynomial expansion of the characteristic speeds $(M \pm 1)$. As observed in Ref. [10], the pressure splitting can be expressed in terms of second-order polynomials $(M \pm 1)^2$ as

$$p_3 : p^{\pm} = \begin{cases} \dfrac{p}{4}(M \pm 1)^2 (2 \mp M), & \text{if } |M| \leqslant 1; \\ \dfrac{p}{2}(M \pm |M|)/M, & \text{otherwise.} \end{cases} \qquad (8a)$$

The other expansion is the simplest possible form of the first order:

$$p_1 : p^{\pm} = \begin{cases} \dfrac{p}{2}(1 \pm M), & \text{if } |M| \leqslant 1; \\ \dfrac{p}{2}(M \pm |M|)/M, & \text{otherwise.} \end{cases} \qquad (8b)$$

In fact, a whole host of choices are possible for the pressure splitting, but with some differences. For example, the first-order polynomial p_1 is non-differentiable at $|M| = 1$. Having tested these two splittings thoroughly, we conclude that both perform admirably. It is interesting to note that the above formulas can be recast in the form

$$\begin{pmatrix} \rho u \\ \rho uu + p \\ \rho uv \\ \rho uH \end{pmatrix}_{1/2} = M_{1/2} \frac{1}{2} \left[\begin{pmatrix} \rho a \\ \rho a u \\ \rho a v \\ \rho a H \end{pmatrix}_L + \begin{pmatrix} \rho a \\ \rho a u \\ \rho a v \\ \rho a H \end{pmatrix}_R \right]$$
$$- \frac{1}{2} |M_{1/2}|\, \Delta_{1/2} \begin{pmatrix} \rho a \\ \rho a u \\ \rho a v \\ \rho a H \end{pmatrix}$$
$$+ \begin{pmatrix} 0 \\ p_L^+ + p_R^- \\ 0 \\ 0 \end{pmatrix}, \qquad (9)$$

where $\Delta_{1/2}\{\bullet\} = \{\bullet\}_R - \{\bullet\}_L$. Here the first term on the RHS is clearly not a simple average of "L" and "R" states, but rather a Mach-number-weighted average. The second term is the numerical dissipation, rendering the flux formula upwinding, and it has merely a scalar coefficient $|M_{1/2}|$, requiring only $O(n)$ operations, in contrast to $O(n^2)$ operations by the Roe matrix. Indeed, a significant saving has been achieved in our explicit code containing both splittings: a factor of about three in the 2D explicit calculation was realized.

The above splitting of both the advective term and pressure term completely define the inviscid flux vector. For
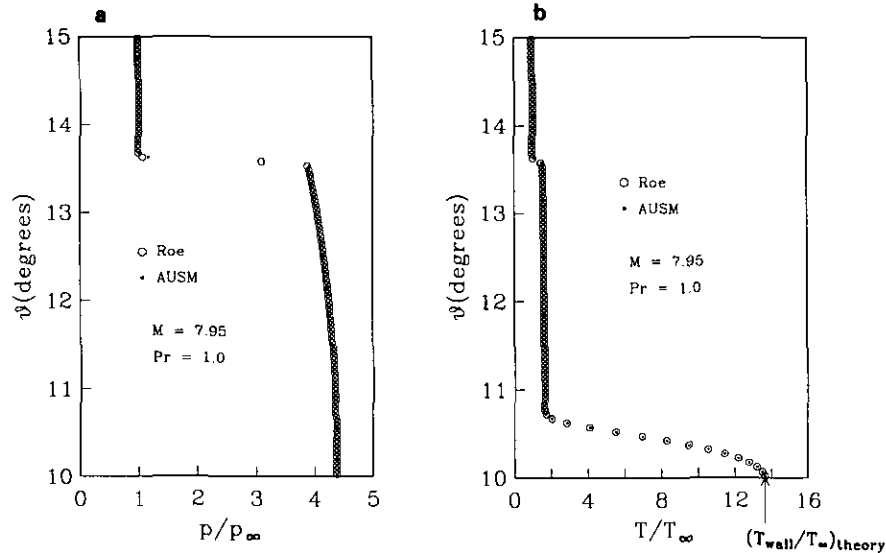
FIG. 4. Hypersonic conical flow, first order accurate results: (a) pressure profile and (b) temperature profile, using the Roe and present splittings.

the viscous terms, the usual central-average representation is used at the interface.

In summary, the new scheme treats the convective and pressure terms separately. The convective terms are upstream-biased using a properly defined cell-interface velocity, while the pressure term is strictly dealt with by using acoustic waves. Accordingly, the name of the scheme is coined as the advection upstream splitting method (AUSM). The method retains the simplicity and efficiency of a FVS scheme. As the following section will bear out, the method also achieves the high level of accuracy attributed only to FDS methods. Furthermore, it has proven thus far to be a robust formulation as a variety of Euler and Navier–Stokes calculations will bear out.

3. RESULTS AND DISCUSSION

Four sets of problems were used to measure the performance of the new splitting technique. First there is the quasi 2D viscous conical flow patterned after the experiments of Van Leer *et al.* [6]. The second set of investigations involved the 2D inviscid calculation about a NACA four-digit series airfoil. These tests were conducted under regimes similar to the GAMM Workshop on the Numerical Simulation of Compressible Euler Flows [12]. The third problem was the shock wave and laminar boundary-layer interaction in which experimental measurements [13] were available for comparison. Finally, the fourth set dealt with a supersonic flow over a circular cylinder for which the Roe scheme is shown to yield anomalous solutions, depending on the Mach number and computation grid.

Case 1. Let us consider a cone of 10°-half angle with a computational domain spanning 5° out from the surface of

the cone. The freestream is defined by a Mach number of 7.95, Reynolds number of 4.2×10^5, stagnation temperature of 775.56 K, and Prandtl number of 1.0. The case of a unity Prandtl number was chosen so that the validation of the present scheme can be performed against the theoretical solution for the adiabatic wall temperature given by

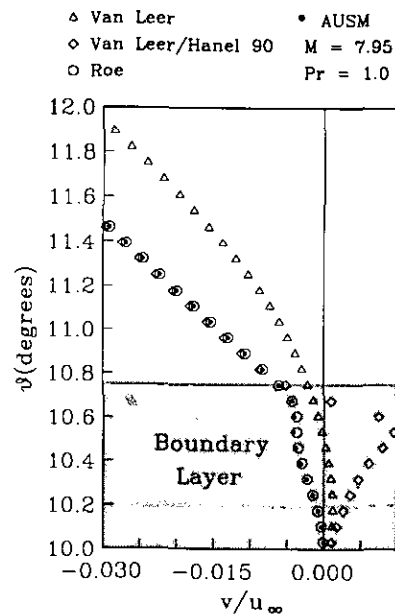$$\frac{T_{wall}}{T_\infty} = 1 + \frac{\gamma - 1}{2} M_\infty^2.$$

FIG. 5. Hypersonic conical flow, first order accurate results: the transverse velocity profiles of all four splittings.
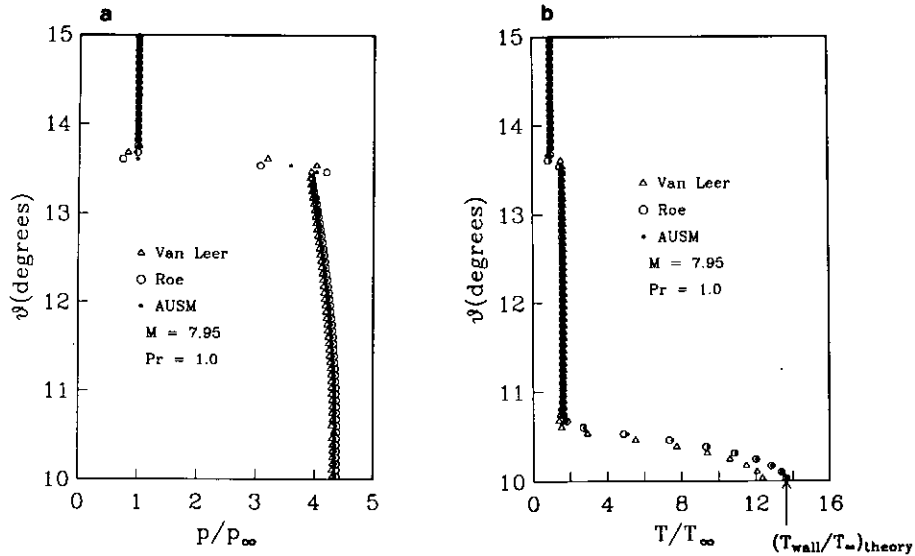
FIG. 6. Hypersonic conical flow, second order accurate results: (a) pressure profile and (b) temperature profile, using the Van Leer FVS, Roe FDS, and AUSM.

First we present first-order results by four techniques. Comparison of the results will clearly show the clue as to why some schemes fail. Next, second-order accurate calculations, using a two-step flux extrapolation procedure [14], were made to prove the stability of the present scheme and the further improvement in accuracy. No limiter is necessary for this case since the shock is relatively weak with a pressure jump being roughly equal to three.

In Figs. 4a and b, the pressure and temperature distributions demonstrate the dramatic improvement by the AUSM from the VLS and related modifications in [8, 9], which were shown earlier in Figs. 3a and b. It is gratifying to see that, while extremely simple, the present AUSM results are

essentially indistinguishable from that of the Roe splitting. Close analysis reveals, in Fig. 5, that the Van Leer scheme and subsequent modifications predict the normal velocity component near the wall with improper sign or value, in comparison with the Roe solution. The pressure irregularity is related to the strong change in the gradient of advective velocity component at the edge of the boundary layer. This suggests that consistent treatment ought be applied to all fluxes, especially the mass flux so that proper balance of velocity components is enforced.

The second-order scheme, shown in Figs. 6a and b, further eliminates any remnant of the glitch in the pressure profile. As usual, the oscillation of the second-order result at
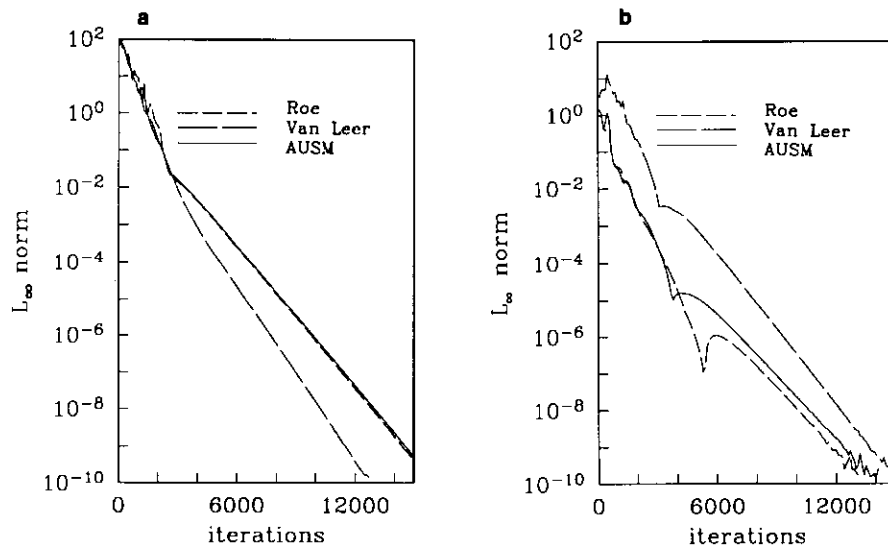

FIG. 7. Hypersonic conical flow, convergence histories: (a) first order and (b) second order schemes.
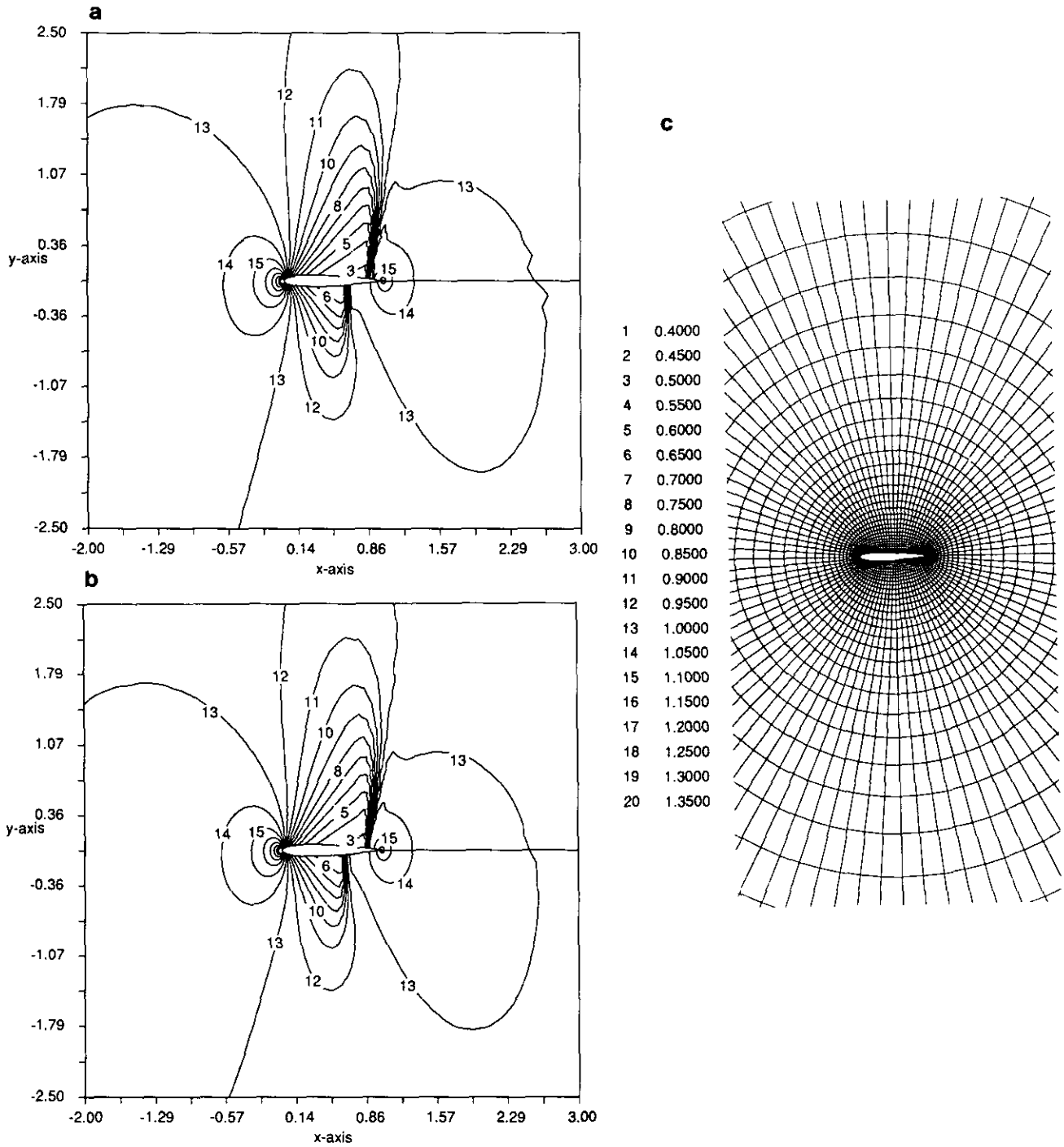
a

b

c

1	0.4000
2	0.4500
3	0.5000
4	0.5500
5	0.6000
6	0.6500
7	0.7000
8	0.7500
9	0.8000
10	0.8500
11	0.9000
12	0.9500
13	1.0000
14	1.0500
15	1.1000
16	1.1500
17	1.2000
18	1.2500
19	1.3000
20	1.3500

FIG. 8. NACA 0012 transonic flow, pressure contours: (a) AUSM and (b) Roe FDS. The 97×33 grid is shown in (c).

the shock can be made to disappear by incorporating a standard TVD scheme. Note that the AUSM gives only very mild oscillations near the shock in the second-order result, weaker than in the Roe solution.

In Figs. 7a and b, convergence history of the first- and second-order calculations for three splittings are shown. They all have more or less the same behavior and slope. However, it seems to indicate that the RS and AUSM are more similar. Also, the convergence rate does not appear deteriorated in the second-order calculations.

Case 2. The NACA 0012 airfoil was chosen for inviscid calculations. The computational domain extends 10 chord lengths out from the half-chord point and is composed of *O*-type 97×33 cells. The code uses an explicit, six-stage Runge–Kutta integration scheme [15]. The finite volume formulation is second-order accurate, but does not include flux limiters. The experiment was conducted under two separate flow conditions: (a) $M_\infty = 0.85$ and angle of attack $(AOA) = 1.0°$: (b) $M_\infty = 1.20$ and $AOA = 0.0°$.

Both cases demonstrate the AUSM as a robust flux-splitting technique. In Figs. 8a, b, and c we present the pressure contours and grid for Case 2a by the AUSM and RS. There is virtually no visible difference between the two solutions; both have accurately captured the upper and lower surface shocks. The solutions have converged at least four orders of magnitude.

The pressure coefficient at both surfaces for Case 2a has also been plotted in Fig. 9 bot both schemes; the lines are for the RS and the symbols for the AUSM. The AUSM appears to be slightly more accurate than Roe's by capturing the inviscid singularity, so called the Zierep singularity, at the foot of the shock on a curved surface. This is manifested by
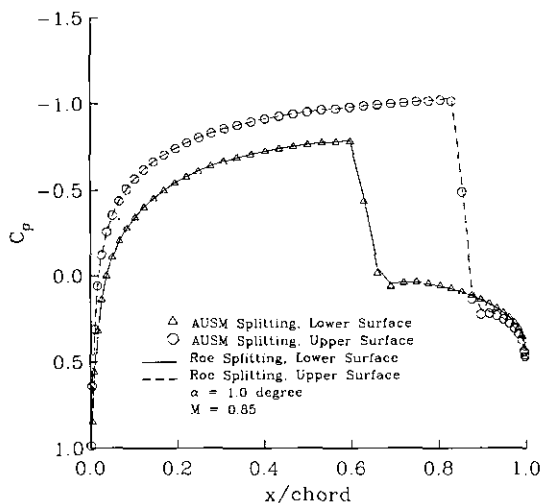

FIG. 9. NACA 0012 transonic flow, surface pressure coefficient.

the overcompression followed by an expansion. However, both shocks are defined in the same number of cells.

The entropy plots for Case 2a are displayed in Figs. 10a and b. It is interesting to note that the entropy generated at the leading edge is about three times weaker in magnitude and confined in a narrower region for the AUSM than the RS.

The pressure plots for Case 2b were presented merely to demonstrate the capability of the AUSM to capture the bow shock and the fishtail shock; the accuracy is evident in Figs. 11a and b. Here, both results are essentially identical.

Up to this point, the Cases 1 and 2 prove that the AUSM is as accurate as the RS. In the next two cases, we will begin to see significant differences, especially in the last case.

Case 3. The experiment by Hakkinen *et al.* [13] at $M_\infty = 2.0$, $Re_\infty = 2.96 \times 10^5$, and shock angle $= 32.58°$ was chosen for calculation using both the AUSM and RS. The computational domain consists of 75×65 grid points. Again no limiter is necessary for the weak shock. Perhaps it should be advised against using the limiter for this problem, in order to minimize unnecessary numerical diffusivity that may overwhelm the physical viscosity. While many calculations have been reported, there are substantial variations among these results as well as from the measurement. In the surface pressure and friction coefficient plots of Figs. 12a and b, we also see significant differences between two splittings. The AUSM gives very good agreement with the data [13] in C_f in the separation as well as reattachment regions (solid dots are the separated region in which C_f was not measured). For the surface pressure plotted in Fig. 12a, the AUSM again produces good agreement with the measurement in the reattachment region, but underpredicts in the separation region. This point is particularly puzzling since the pressure rise and the drop in skin friction should go hand in hand. There is no apparent reason that a prediction coincides with the C_f, but not with P. However, the ability of obtaining good agreement of the reattachment with the data is worth noting since it is usually harder to achieve this than to predict separation. Further investigation of the experiment is clearly useful, but this is beyond the scope of the present paper. Insofar as the uncertainty in the measurements, it is hard to draw definitive judgment regarding the accuracy of both schemes. Figures 13a and b display the Mach contours; the AUSM results seem to give a sharper definition of the incoming oblique shock as well as the complex expansion/compression waves in the interaction region. We note that residuals have dropped five orders of magnitude in both calculations.

Case 4. The 2D supersonic flow over a circular blunt body was chosen to demonstrate the ability of the AUSM to correctly resolve the strong bow shock and the acceleration of stagnant flow through a sonic point to supersonic speed.
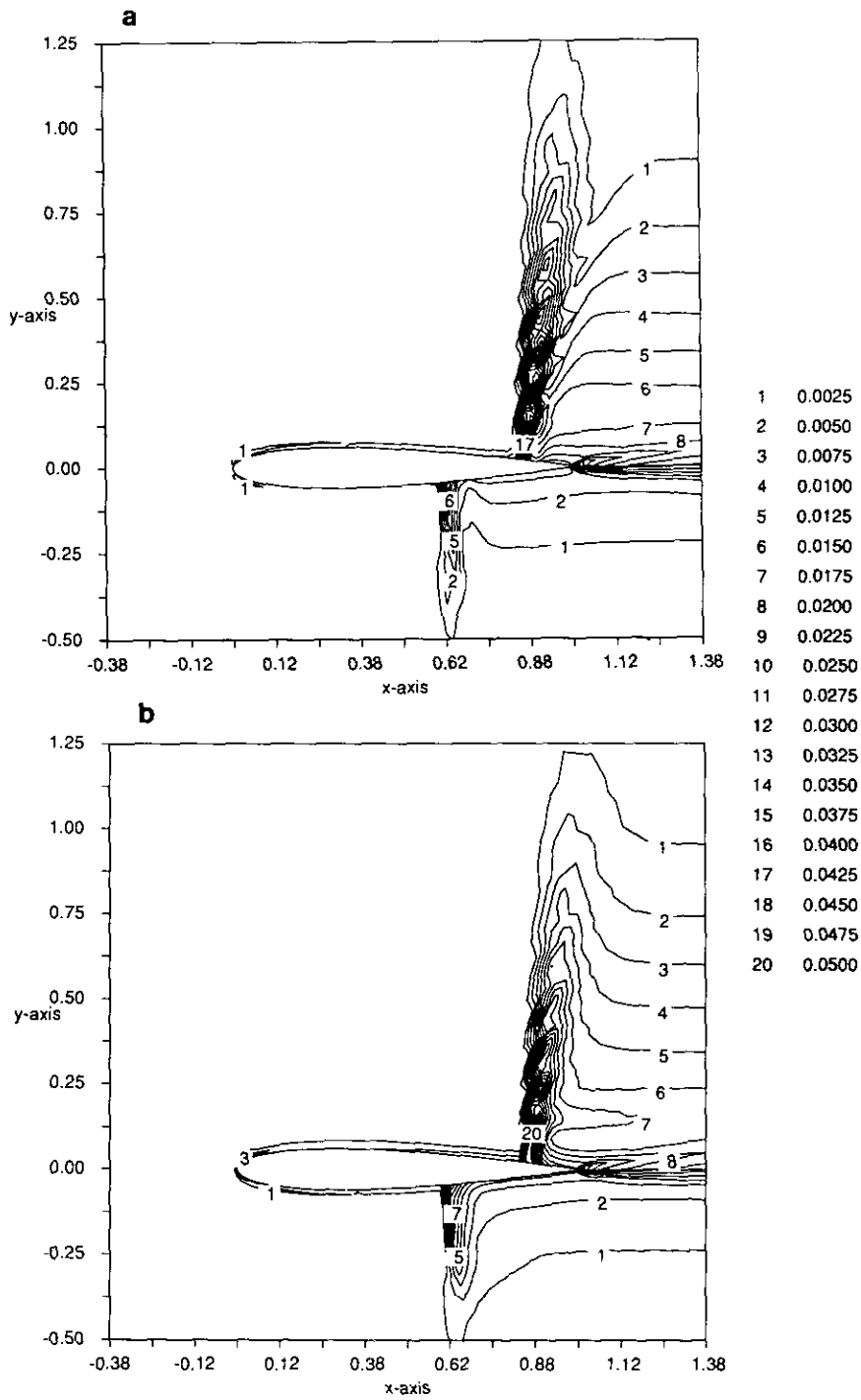
FIG. 10. NACA 0012 transonic flow, entropy contours: (a) AUSM and (b) Roe FDS.
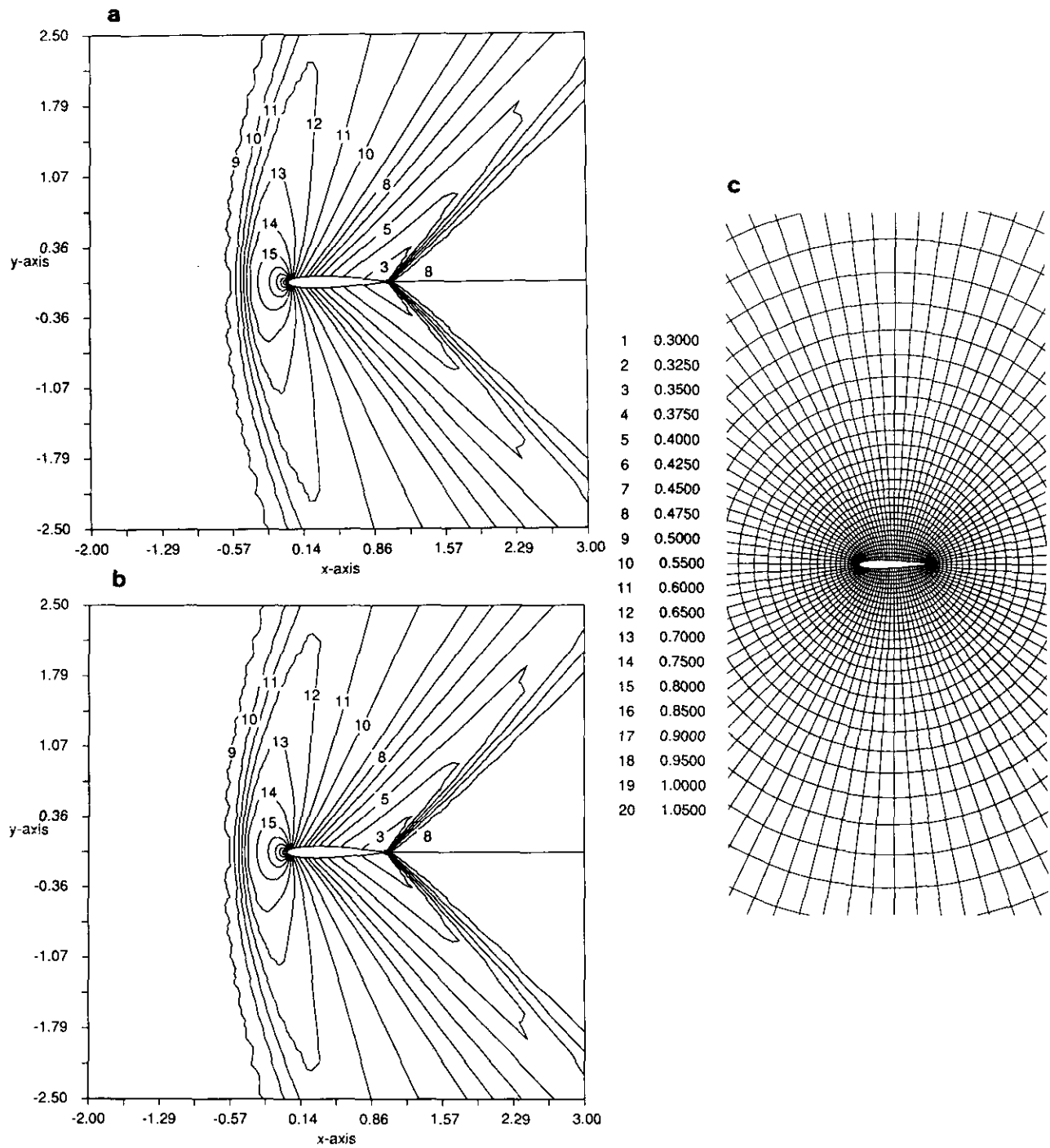
LIOU AND STEFFEN

1	0.3000
2	0.3250
3	0.3500
4	0.3750
5	0.4000
6	0.4250
7	0.4500
8	0.4750
9	0.5000
10	0.5500
11	0.6000
12	0.6500
13	0.7000
14	0.7500
15	0.8000
16	0.8500
17	0.9000
18	0.9500
19	1.0000
20	1.0500

FIG. 11. NACA 0012 supersonic flow, pressure contours: (a) AUSM and (b) Roe FDS. The 97×33 grid is shown in (c).
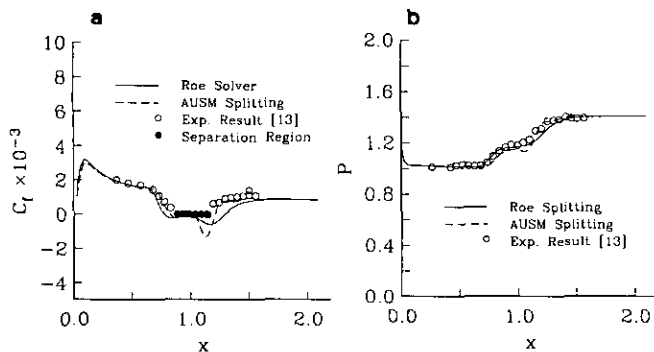
FIG. 12. Shock wave and boundary layer interactions: (a) skin friction coefficient and (b) surface pressure, of the Roe FDS and AUSM solutions in comparison to experimental data [13].

The first-order results are given for this problem. A range of free-stream Mach numbers from 2 to 20 were calculated along with the study of grid effect on the solution. The results presented were obtained from two types of grids: (1) 57×33 circular grid with stretching in the radial direction and (2) 45×43 shock-aligned grid with uniform radial spacing; they are displayed together with the Mach number contours for the calculations to be presented.

As reported recently by Peery and Imlay [16] and Lin [17], Roe's splitting produced anomalous solutions that were manifested by odd-shaped bow shocks. This non-physical solution, sometimes referred to as the "carbuncle phenomenon," is not completely understood yet. Nevertheless, fixes are available in Refs. [16, 17] and involve empiricism and smoothing which amounts to adding an extra dose of numerical dissipation. In our calculations, three types of "carbuncle phenomena" have been observed in the contours. They are nonsymmetric, protuberant, and indented. The solutions appeared to be grid and Mach number dependent. Several different Mach numbers were examined on several different grids. In the following, we show some typical results obtained by the Roe splitting and AUSM. The first-order results are shown to compare the minimum capability of each scheme for this type of problem. Second-order results (not included) using the AUSM also have been obtained free from the "carbuncle phenomena" and showed improvement of accuracy.

Figures 14a and b give the comparison of Mach contours for $M_\infty = 6.0$ along with the grid in Fig. 14c. For the RS, a protuberant shock is stopped at the outer boundary and a nonsymmetric flow is developed near the stagnation point. A velocity vector plot in this enlarged region, Fig. 13d shows a complex but nonphysical flow pattern. The AUSM, on the other hand, results in a smooth symmetric shock shape. It is noted that all results reported for this case have been obtained with residual dropped more than five decades for both schemes.

Figures 15a and b display the results for $M_\infty = 4.0$ for the circular grid shown in 15c. The RS yields a nonsymmetric flow while the AUSM converges to a completely symmetric solution. However, a slight irregularity seen on the sonic line was attributed to the use of the pressure splitting, p_3 in (8a). Close investigation of the staircase contours in the curved part of the shock revealed that they are largely due to the nonalignment of the shock with the circular grid (Fig. 15c). This effect disappears as the grid is aligned with the shock, as seen in the previous test, Figs. 14.

A change of the Mach number to $M_\infty = 3.0$ on the same grid resulted in a different type of contour in the RS calculation. Indented but symmetric contours, Fig. 16b, were developed. This shows the sensitivity of the RS solution to the flow condition. Again, the AUSM gives the correct behavior, except a slight glitch on the sonic line due to the p_3 splitting.

Finally, we show how the solution for $M_\infty = 6.0$ (see Fig. 14) changes when the grid of Fig. 15 is used. In Figs. 17, the RS solution changed to the indented type from the opposite, protuberant type. Once again, the AUSM behaved rather commendably.

In this paper, we have restricted our attention to the performance of the current method for the steady-flow calculations. Preliminary study of the shock-tube problem, e.g., Sod problem, indicates minor difficulty that arises at startup of the calculation. A quick fix can be prescribed by, for example, either lowering the time step or using other splittings initially. At later times, the results are comparable to those from the Roe splitting. A comprehensive development of the method with emphasis to unsteady flows will be reported in a companion paper.

4. CONCLUDING REMARKS

As guided by physical intuition and mathematical property, we propose a new flux splitting formula, AUSM, that uses a properly defined advection velocity to determine an upstream extrapolation at the cell interface. The scheme is remarkably simple, requiring only $O(n)$ operation, and renders itself for an easy implementation in a code. Furthermore, it is at least as accurate as the Roe solver for the problems tested. In the blunt body problem, the AUSM resulted in correct solutions without difficulty in every test in a wide variation of flow conditions and grids, where the Roe splitting failed. The above promising features should make the new scheme very suitable for a calculation requiring both efficiency and accuracy, e.g., in the case of Navier–Stokes or chemical reacting flows. Our search for an alternative splitting that will meet the goals of efficiency, accuracy, and robustness does suggest that there are sufficient possibilities for further success.
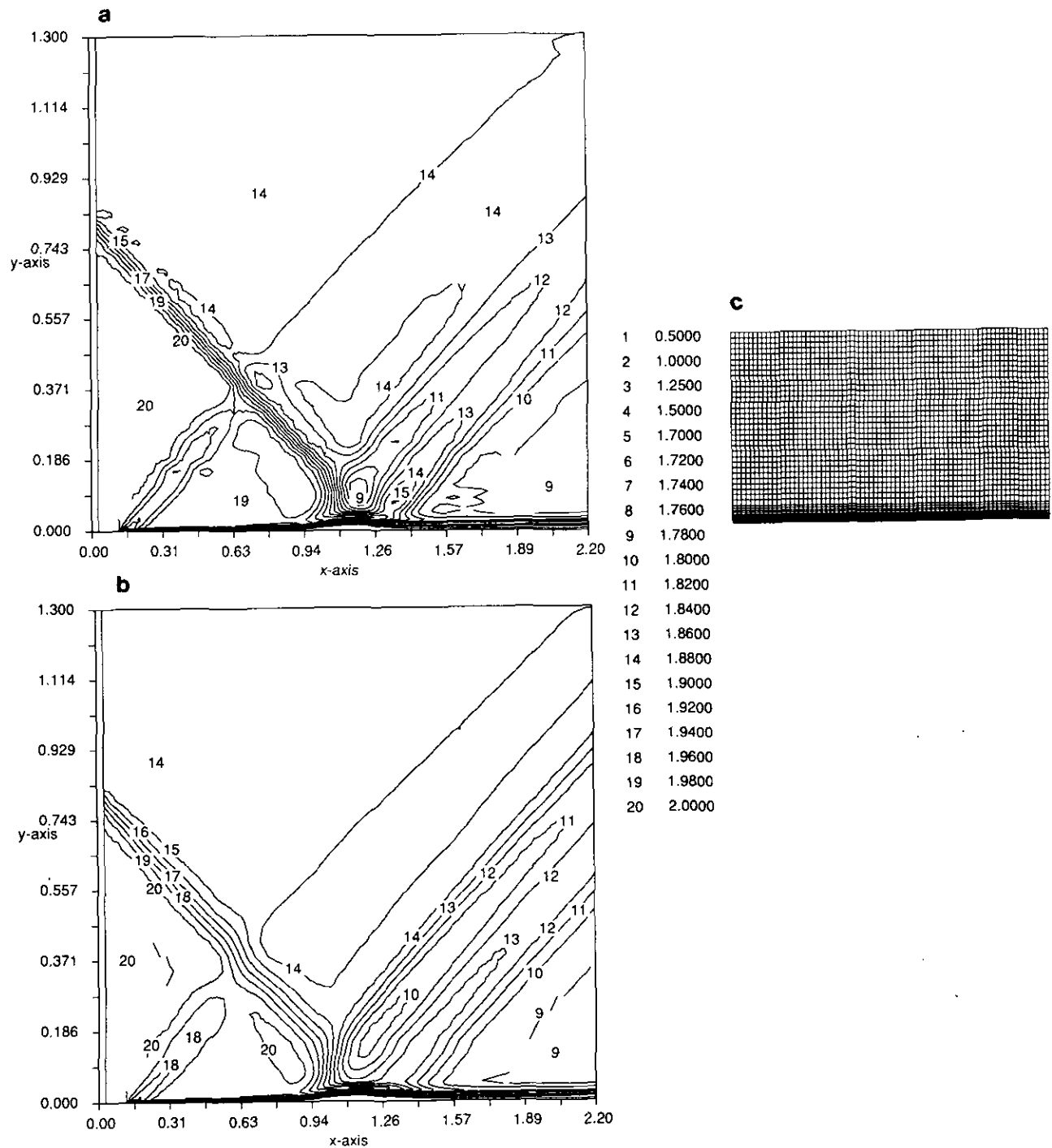
FIG. 13. Shock wave and boundary layer interaction, Mach contours: (a) AUSM and (b) Roe FDS. The 75×65 grid is shown in (c).

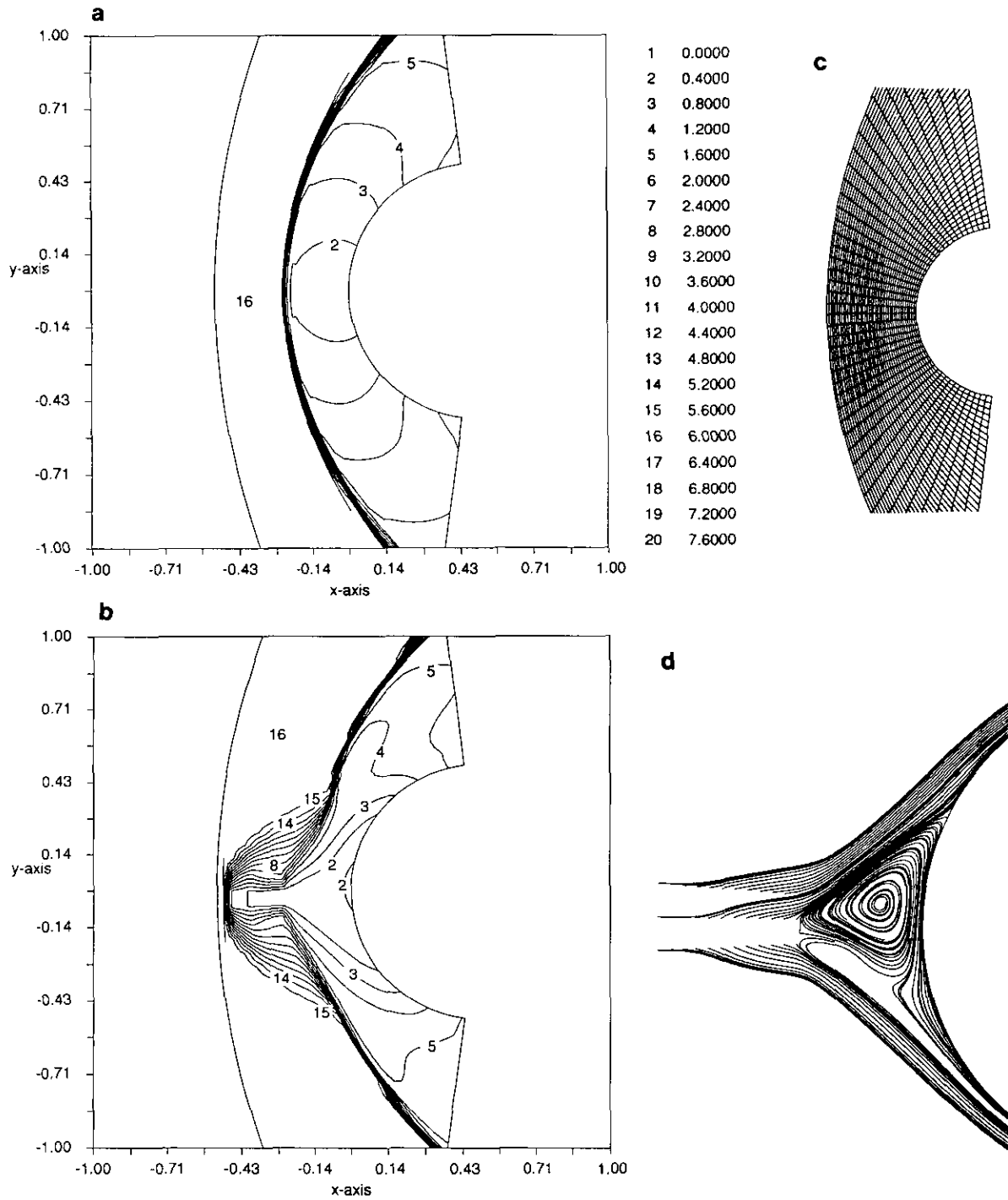| 1 | 0.0000 |
2	0.4000
3	0.8000
4	1.2000
5	1.6000
6	2.0000
7	2.4000
8	2.8000
9	3.2000
10	3.6000
11	4.0000
12	4.4000
13	4.8000
14	5.2000
15	5.6000
16	6.0000
17	6.4000
18	6.8000
19	7.2000
20	7.6000

FIG. 14. Mach 6.0 flow over a circular cylinder, Mach contours: (a) AUSM and (b) Roe FDS. The 45 × 43, shock aligned grid is shown in (c). The particle traces shown in (d) also demonstrate the nonphysical nature of the Roe solution, corresponding to (b).
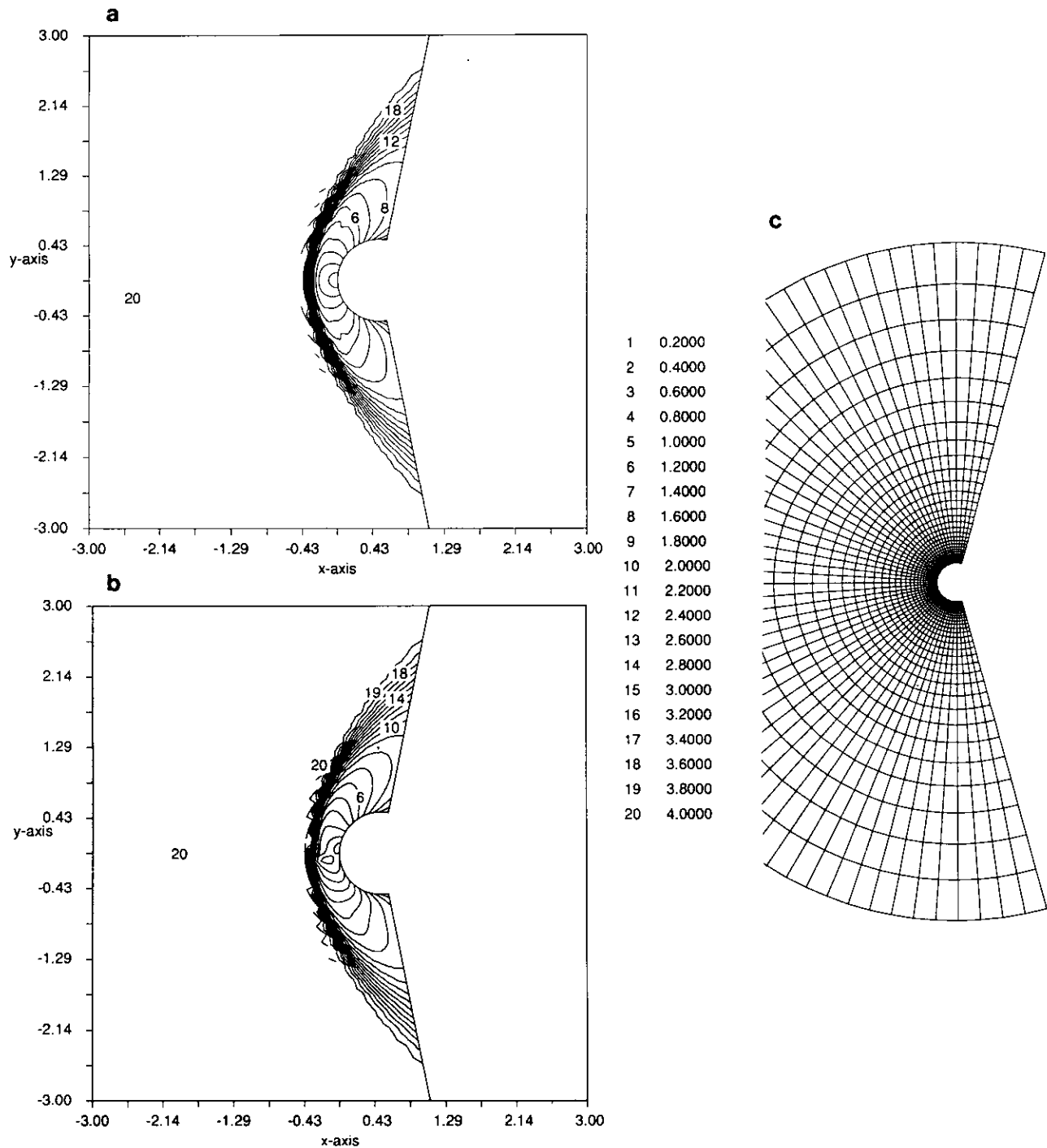
1	0.2000
2	0.4000
3	0.6000
4	0.8000
5	1.0000
6	1.2000
7	1.4000
8	1.6000
9	1.8000
10	2.0000
11	2.2000
12	2.4000
13	2.6000
14	2.8000
15	3.0000
16	3.2000
17	3.4000
18	3.6000
19	3.8000
20	4.0000

FIG. 15. Mach 4.0 flow over a circular cylinder, Mach contours: (a) AUSM and (b) Roe FDS. The 57 × 33, radially stretched circular grid is shown in (c).
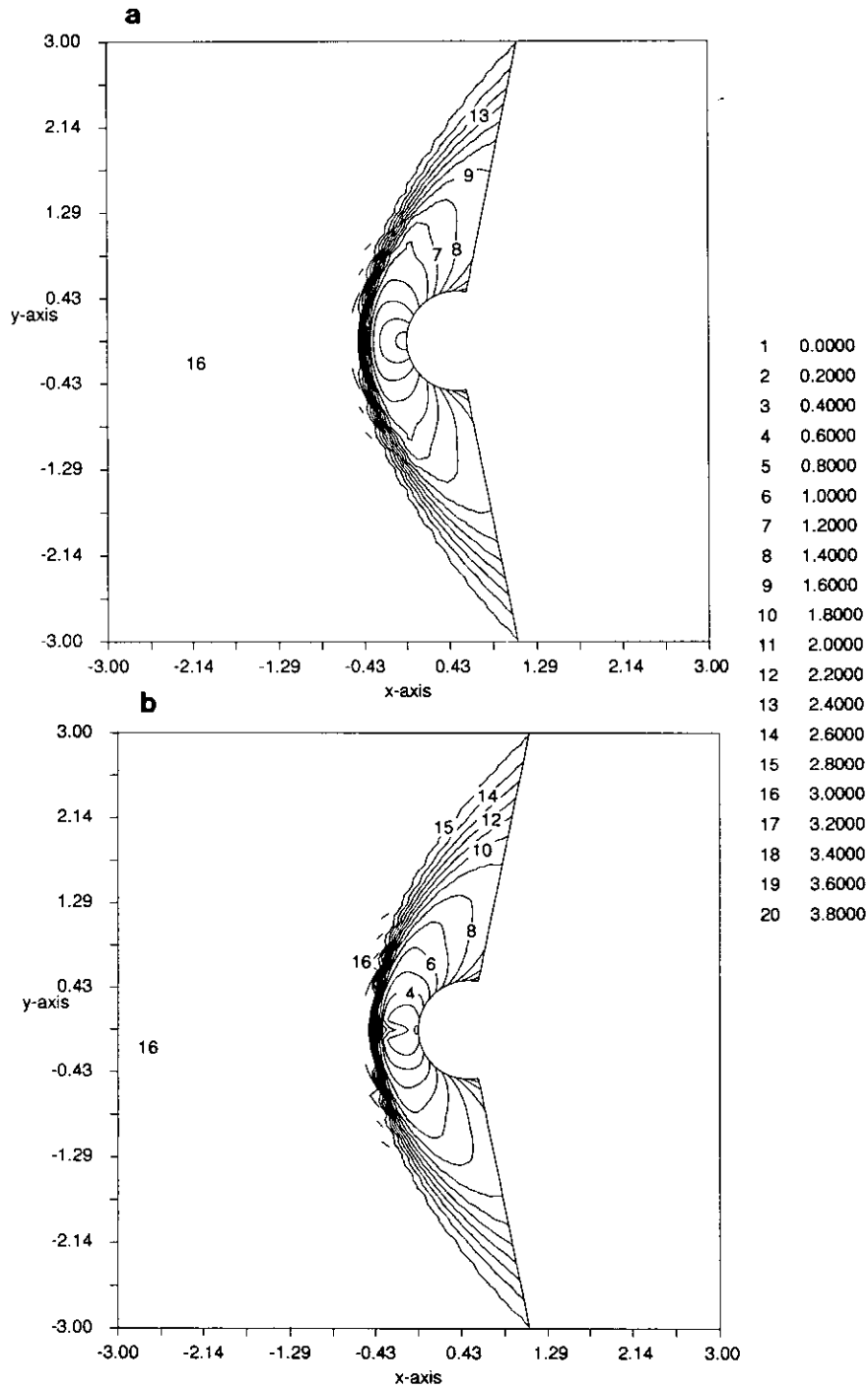
FIG. 16. Mach 3.0 flow over a circular cylinder, Mach contours: (a) AUSM and (b) Roe FDS. Same grid as in Fig. 15.
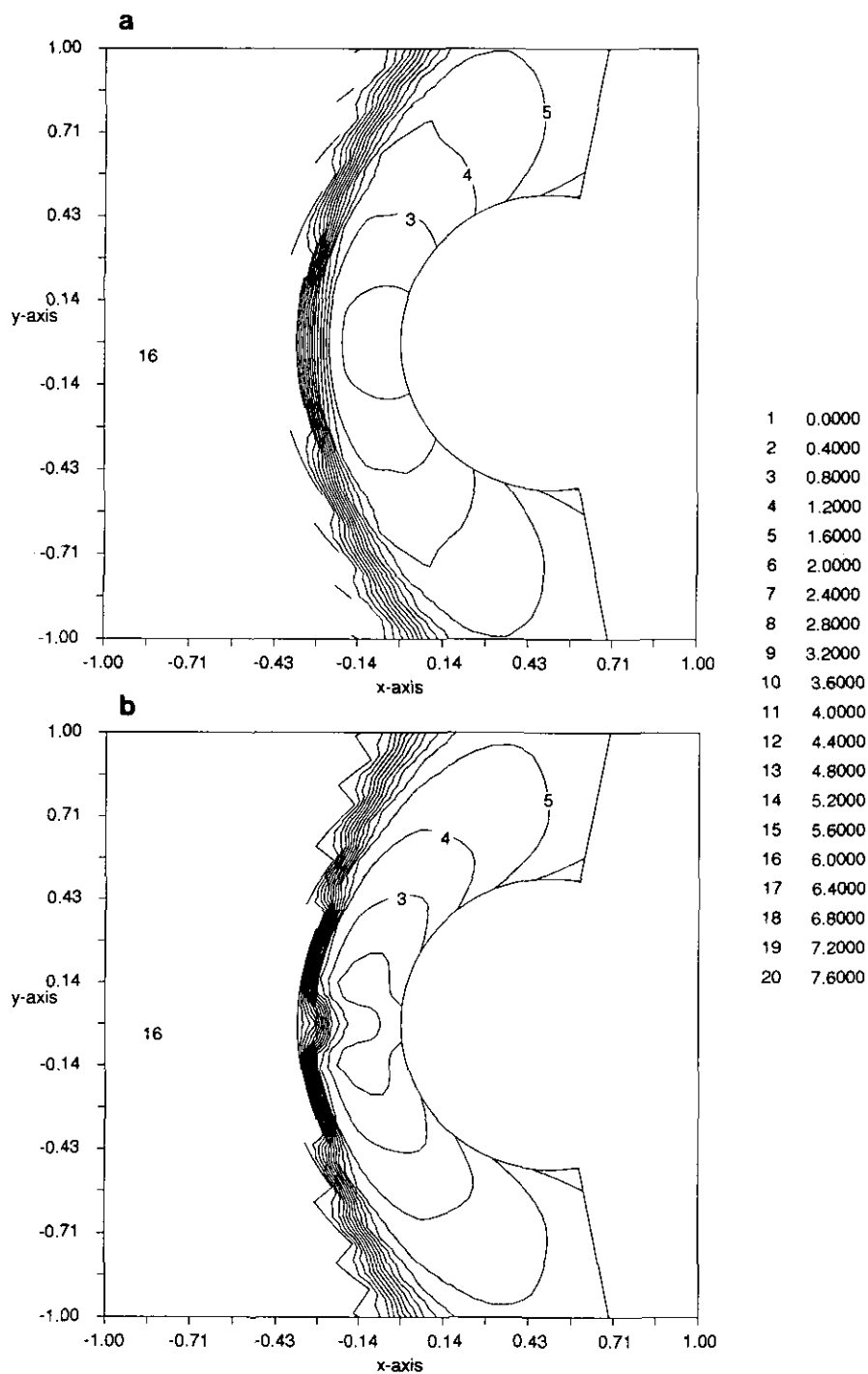
1	0.0000
2	0.4000
3	0.8000
4	1.2000
5	1.6000
6	2.0000
7	2.4000
8	2.8000
9	3.2000
10	3.6000
11	4.0000
12	4.4000
13	4.8000
14	5.2000
15	5.6000
16	6.0000
17	6.4000
18	6.8000
19	7.2000
20	7.6000

FIG. 17. Mach 6.0 flow over a circular cylinder, Mach contours: (a) AUSM and (b) Roe FDS. Same grid as in Fig. 15.

ACKNOWLEDGMENTS

REFERENCES

1. M.-S. Liou and B. van Leer, AIAA Paper 88-0624, 1988 (unpublished).

2. B. Koren, *J. Comput. Phys.* **87**, 25 (1990).

3. A. Suresh and M.-S. Liou, *AIAA J.* **29**, 920 (1991).

4. A. Suresh and M.-S. Liou, The Osher scheme for non-equilibrium reacting flows, *Int. J. Numer. Methods Fluids* **15**, 219 (1992).

5. B. van Leer, *Lecture Notes in Physics*, Vol. 170 (Springer-Verlag, New York/Berlin, 1982), p. 507.

6. B. van Leer, J. L. Thomas, P. L. Roe, and R. W. Newsome, AIAA Paper 87-1104, 1987 (unpublished).

7. D. Hänel, R. Schwane, and G. Seider, AIAA Paper 87-1105, 1987 (unpublished).

8. D. Hänel and R. Schwane, AIAA Paper 89-0274, 1989 (unpublished).

9. B. van Leer, NASA CP-3078, p. 203, 1991 (unpublished).

10. M.-S. Liou, B. van Leer, and J.-S. Shuen, *J. Comput. Phys.* **87**, 1 (1990).

11. M.-S. Liou and C. J. Steffen, Jr., NASA TM 104452, 1991 (unpublished).

12. GAMM Workshop on the Numerical Simulation of Compressible Euler Flows, June 1986.

13. R. J. Hakkinen, I. Greber, L. Trilling, and S. S. Abarbanel, NASA Memo 2-18-59W, 1959 (unpublished).

14. C. Hirsch, *Numerical Computation of Internal and External Flows, Vol. 2* (Wiley, New York, 1990), p. 495.

15. B. van Leer, C.-H. Tai, and K. G. Powell, AIAA Paper 89-1933, 1989 (unpublished).

16. K. M. Perry and S. T. Imlay, AIAA Paper 88-2904, 1988 (unpublished).

17. H.-C. Lin, AIAA Paper 91-1544, 1991 (unpublished).

18. W. J. Coirier and B. van Leer, AIAA Paper 91-1566, 1991 (unpublished).

19. P. L. Roe, ICASE Report 84-53, 1984 (unpublished).